

## Metabolic topography of autoimmune non-paraneoplastic encephalitis

Madhavi Tripathi<sup>1</sup> · Manjari Tripathi<sup>2</sup> · Shambo Guha Roy<sup>1</sup> · Girish Kumar Parida<sup>1</sup> · Kavish Ihtisham<sup>2</sup> · Deepa Dash<sup>2</sup> · Nishikant Damle<sup>1</sup> · Shamim Ahmed Shamim<sup>1</sup> · Chandrasekhar Bal<sup>1</sup>

Received: 20 April 2017 / Accepted: 28 November 2017 / Published online: 18 December 2017  
© Springer-Verlag GmbH Germany, part of Springer Nature 2017

### Abstract

**Purpose** F-18 fluorodeoxyglucose (FDG) positron emission tomography (PET) is emerging to be a useful tool in supporting the diagnosis of AIE. In this study, we describe the metabolic patterns on F-18 FDG PET imaging in AIE.

**Methods** Twenty-four antibody-positive patients (anti-NMDA-15, anti-VGKC/LGI1-6, and anti-GAD-3), 14 females and 10 males, with an age range of 2–83 years were included in this study. Each PET study was evaluated visually for the presence of hypometabolism or hypermetabolism and semiquantitatively using Cortex ID (GE) and Scenium (Siemens) by measuring regional Z-scores. These patterns were correlated with corresponding antibody positivity once available.

**Results** Visually, a pattern of hypometabolism, hypermetabolism, or both in various spatial distributions was appreciated in all 24 patients. On quantitative analysis using scenium parietal and occipital lobes showed significant hypometabolism with median Z-score of -3.8 (R) and -3.7 (L) and -2.2 (R) and -2.5 (L) respectively. Two-thirds (16/24) showed significant hypermetabolism involving the basal ganglia with median Z-score of 2.4 (R) and 3.0 (L). Similarly on Cortex ID, the median Z-score for hypometabolism in parietal and occipital lobes was -2.2 (R) and -2.4 (L) and -2.6 (R) and -2.4 (L) respectively, while subcortical regions were not evaluated. MRI showed signal alterations in only 11 of these patients.

**Conclusion** There is heterogeneity in metabolic topography of AIE which is characterized by hypometabolism most commonly involving the parietal and occipital cortices and hypermetabolism most commonly involving the basal ganglia. Scenium analysis using regional Z-scores can complement visual evaluation for demonstration of these metabolic patterns on FDG PET.

**Keywords** F-18 FDG · AIE · NMDAR · LGI1 · GAD · PET

### Introduction

In recent years, autoimmune encephalitis (AIE) with antibodies directed against cell-surface antigens has been increasingly recognized [1]. In contrast to the classic paraneoplastic syndrome of limbic encephalitis (LE) with onconeural antibodies, they occur with or without an underlying tumor and frequently respond well to immunotherapy [2, 3]. Owing to the variety of antibodies against different cell surface proteins/ion

channels, patients with AIE may present with a variety of symptoms and neuroimaging features [1].

A diagnostic workup suggesting possible autoimmune encephalitis enables timely initiation of immunotherapy and patients generally respond well to treatment. The initial workup includes conventional neurological evaluation and standard diagnostic tests such as magnetic resonance imaging (MRI), CSF analysis, and EEG [1]. Antibody testing further establishes the diagnosis of probable AIE or definite AIE thus enabling refinement of treatment protocols [1]. Though signal changes on MRI have been included in the diagnostic algorithm of AIE, it has been shown that a significant fraction (37.5 to 89%) of patients with AIE may have a normal MRI initially [4, 5]. Early in the disease process, fluorodeoxyglucose (FDG) positron emission tomography (PET) appears to be a more sensitive imaging modality for detecting temporal lobe abnormalities with normal brain MR imaging [4, 6, 7].

✉ Madhavi Tripathi  
madhavi.dave.97@gmail.com

<sup>1</sup> Department of Nuclear Medicine, All India Institute of Medical Sciences, New Delhi 110029, India

<sup>2</sup> Department of Neurology, Cardiothoracic and Neurosciences Centre, All India Institute of Medical Sciences, New Delhi, India

FDG PET studies in patients with antibodies against intracellular antigens has demonstrated mesial temporal hypermetabolism [4, 8–11] while in AIE with antibodies directed against the surface antigens cortical involvement has also been described [12–19]. We undertook this analysis to evaluate the metabolic patterns of AIE imaged with F-18 FDG PET.

## Materials and methods

This observational case series included the FDG PET scans of 24 patients with antibody-positive AIE, imaged between January 2015 and January 2017. Patients were referred by the treating neurologist and underwent FDG PET and MRI as part of their diagnostic work-up for AIE. The diagnostic work-up protocol for AIE was approved by the institute's ethics committee and informed consent was taken from each patient.

AIE was suspected because of the subacute onset of neurological symptoms which included short-term memory loss, behavioral problems, extrapyramidal symptoms, sleep disturbance, or seizures. The presence of an underlying malignancy was excluded by whole body PET/CT in all included cases. Steroids were not started in any patient prior to the diagnostic work-up. Subsequent diagnosis of AIE was confirmed with antibody positivity and response to immunotherapy.

The median time between onset of symptoms and FDG PET was 12 weeks (range from 4 to 96 weeks). This delay was mostly because the patients had initially been evaluated in outside centers and were subsequently referred to our tertiary care hospital.

**Procedure** PET/CT was performed approximately 60 min after intravenous injection of 222–296 MBq (6–8 mCi) of F-18 FDG. Imaging was performed on a Biograph mCT (Siemens, Erlangen, Germany). Initial scout of the head was followed by non-contrast CT acquisition (110 mA, 120 kVp) for attenuation correction and anatomical co-registration. This was followed by a single bed, 3-D PET emission scan for 10 min. PET images were reconstructed (ultra HD-PET) by iterative reconstruction (5 iterations and 21 subsets). A whole-body protocol was also acquired to rule out systemic malignancy. In patients with a history of seizures, a 32 channel EEG monitoring was carried out during the FDG uptake phase.

**Image interpretation** The FDG-PET images were interpreted visually on a MMWP workstation (Siemens) by a nuclear medicine physician with experience (10 years) in reading brain FDG-PET images. Image patterns were classified into three broad subgroups: (1) with hypermetabolism only, (2) with hyper and hypometabolism, and (3) with

hypometabolism only. Further the spatial distribution pattern was detailed in each case.

Each case was further analyzed using Cortex ID (GE Healthcare, Waukesha, WI) on a Xeleris workstation and Scenium (Siemens Molecular Imaging Limited) on the MMWP workstation. Both applications involve generation of brain maps which were compared with a commercially available comprehensive database of normal brain scans, and normalized to the pons. Automated voxel-by voxel Z-scores were generated for the following region of interest (ROI): right and left parietal, frontal, lateral temporal, mesial temporal and occipital cortices, and cerebellum. In addition, Scenium enabled generation of Z-scores for the basal ganglia. [Z-score = (mean subject-mean database) / standard deviation database]. The voxel-based color-coded statistical analysis of average Z-scores displayed the magnitude of metabolic change for each region. A Z-score threshold of > 2, corresponding to a *p* value of 0.05 (two-tail), was applied for demarcation of significant abnormalities; negative Z-scores indicate hypometabolism. All values were validated by visual inspection also.

MRI was performed using a 32-channel head coil on a 3 T Acheiva/Ingenia system (Philips, Healthcare). The following sequences were acquired: axial T1-weighted (w) (TR/TE, 600/10 ms), T2 w (TR/TE 3000/80 ms), with a flip angle of 90°, and axial FLAIR (TR/TI 11,000/2800 ms and 125 ms); slice thickness 4 mm; with voxel size 0.5 × 0.5, matrix 540 × 360; FOV 230 (AP) × 183 (RL) × 134 (FH). DWI was performed using *b* values of 0 and 1000.

## Results

Baseline characteristics of the 24 patients are summarized in Table 1; 14 were female and 10 were male. Age ranged from 2 to 83 years.

Metabolic abnormalities identified were classified on the basis of antibody positivity. The final diagnosis of AIE was made by the neurologist on getting the results of the antibody panel and response to immunotherapy.

### NMDA receptor antibody encephalitis

Sixteen patients, aged 2 to 63 years, were found to be NMDA receptor (NMDAR) antibody positive. All patients were found to have an abnormal pattern of FDG uptake on visual and semi-quantitative evaluation.

Pattern 1 (four patients): Hypermetabolism involving the lateral temporal cortices (Fig. 1a, b) was seen in two patients, involving both basal ganglia and occipital cortices in combination (Fig. 1c) in one patient and the mesial temporal/hippocampal cortices and basal ganglia, in one patient.

**Table 1** Summary of baseline characteristics of the 24 patients

S No	Age	Gender	Antibody	Interval between first symptom and PET imaging (weeks)	Hypometabolism on FDG PET	Hypometabolism on FDG PET	MRI	Clinical presentation
1	9	M	NMDA	6	b/l basifrontal b/l BG + occipital	Cerebellar + MT	N	Seizures
2	2	F	NMDA	16				Seizures with extrapyramidal features
3	25	F	NMDA	8	b/l hippocampus + BG			
4	23	M	NMDA	10	Caudate	PO + cerebellum b/l P + T + O + cerebellar b/l PO	N	Seizures
5	2	M	NMDA	12			N	Seizures + behavioral changes
6	4	F	NMDA	6	BG		N	Seizures + behavioral issues + oral dyskinesia
7	17	F	NMDA	20	BG + th + PCC + midbrain	Cerebellum	N	Seizures with aggression
8	6	M	NMDA	6	Patchy hypometabolism in right frontal + BG	T2 hyperintensities in rt external capsule and adjoining putamen of basal ganglia and in subcortical white matter in right frontal lobe		
9	26	M	NMDA	96		Cortical		Parkinsonism
10	15	F	NMDA	12	Lateral temp			
11	14	F	NMDA	20	BG	Parieto-occipital	Temp hyperintensities	Seizures
12	19	F	NMDA	18	BG	Parieto-occipital	N	Seizures
13	23	F	NMDA	14		Parieto-occipital	N	Seizures
14	20	F	NMDA	4		Left hemispheric	bl mesial temporal hyperintensity	Behavior + psychiatric issues
							T2 and flair hyperintensities in posterior limb of left internal capsule	Behavioral issues + limb and gait apraxia
15	63	M	NMDA	5		Cerebellum	N	
16	28	F	NMDA	4	STG		N	Ataxia
17	61	M	LGI	8	BG + Th	b/l P + F + T + PC	N	Cognitive decline
18	83	F	LGI	6	BG		N	Rapidly progressive dementia
19	40	F	LGI	14	b/l BG + MT + ACC		N	FBDS
20	66	M	LGI	12	MT + caudate		N	Seizure
21	45	M	LGI	8	b/l BG + MT		N	Recent onset memory loss
22	55	F	GAD	12	b/l MT + BG	P + T	N	Cognitive decline
								Acute onset behavioral disturbance
23	75	F	GAD	20	BG		N	
24	30	M	GAD	24		Cerebellum		Cognitive complaints + gait ataxia
								Symmetrical gait ataxia

F frontal, PO parieto-occipital, BG basal ganglia, P parietal, T temporal, O occipital, Th thalamus, MT mesial temporal, PCC posterior cingulate cortex, b/l bilateral, STG superior temporal gyrus, ACC anterior cingulate cortex

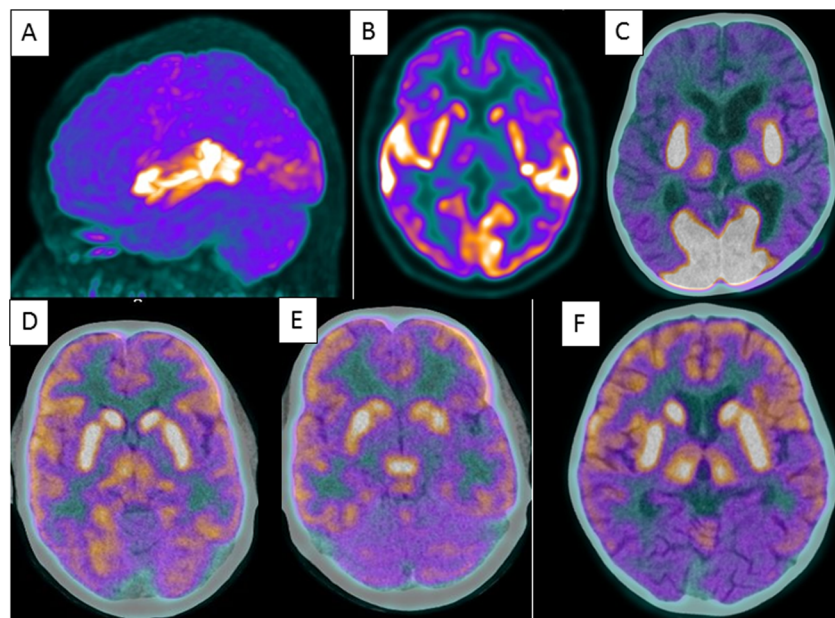


**Fig. 1** **a, b** Sagittal MIP and plain F-18 FDG PET images in a 28/F with cognitive decline and NMDAR antibody positive reveals a ribbon-like pattern of hypermetabolism in both superior temporal gyri. **c** 2/F with a history of seizures, fused transaxial F-18 FDG PET/CT images reveal hypermetabolism in both basal ganglia and occipital lobes. She was NMDAR antibody positive. **d, e** Fused F-18 FDG PET/CT images in a

17/F with oral dyskineticas and abnormal behavior found to be NMDAR antibody positive, reveal hypermetabolism in both basal ganglia and mid-brain **f** 4/F with a history of seizures, positive for NMDAR antibodies, fused F-18 FDG PET/CT images reveal hypermetabolism in both basal ganglia with hypometabolism in the temporo-parieto-occipital cortices (fronto-occipital gradient)

**Pattern 2** (six patients): The hyper-hypometabolism pattern consisted of hypermetabolism involving the basal ganglia, mid-brain (Fig. 1d, e) and basifrontal regions with hypometabolism involving predominantly the parieto-occipital cortices (Fig. 1f) with or without cerebellar hypometabolism.

**Pattern 3** (six patients): Predominant hypometabolism was seen involving the parieto-temporo-occipital cortices. One patient had hemispheric (left-side) hypometabolism, in one it was patchy involving right frontal cortices and right basal ganglia (Fig. 2a, b), and in another it was generalized (Fig. 2c).

#### Voltage-gated potassium channel (VGKC)/leucine-rich glioma inactivated 1 antibody encephalitis

We had five patients in this group; all patients demonstrated an abnormal metabolic pattern on visual and semi-quantitative evaluation. Four patients showed type 1 pattern (predominant hypermetabolism), one patient had basal ganglia hypermetabolism and she presented with bilateral faciobranchial dystonic seizures (FBDS); this case has been reported previously [20]. The second patient with right-sided FBDS had hypermetabolism involving both mesial temporal cortices and left caudate (Fig. 3a, b). The third and fourth cases had hypermetabolism involving both mesial temporal cortices and basal ganglia and anterior cingulate cortices (one case).

**Pattern 2:** One patient had basal ganglia and thalamic hypermetabolism with hypometabolism in right parietal, right

frontal, temporal, and posterior cingulate cortices (Fig. 3c, d). This patient was VGKC antibody positive.

#### Anti-glutamic acid decarboxylase receptor antibody pattern

- Pattern 1. Basal ganglia and brainstem hypermetabolism (Fig. 4a, b) was seen in one case.
- Pattern 2. One patient had bilateral basal ganglia and mesial temporal hypermetabolism with parieto-temporal hypometabolism.
- Pattern 3. One patient had only cerebellar hypometabolism (Fig. 4c).

Semi-quantitative analysis revealed significant metabolic change in at least one cortical or subcortical ROI in all patients. Median and interquartile range of Z-scores on Scenium are shown in Fig. 5 (box and whisker plot). Significant hypometabolism ( $Z\text{-score} < -2$ ) was observed involving both parietal lobes and occipital lobes with median Z-score of  $-3.8$  (R) and  $-3.7$  (L) and  $-2.2$  (R) and  $-2.5$  (L) respectively. Significant hypermetabolism ( $Z\text{-score} > 2$ ) was observed in 16/24 patients (66%) most commonly involving the basal ganglia, Z-score 2.4 (R) and 3.0 (L). Median Z-score for the temporal cortices was not significant; however, the individual Z-scores for the lateral temporal cortices in two patients who

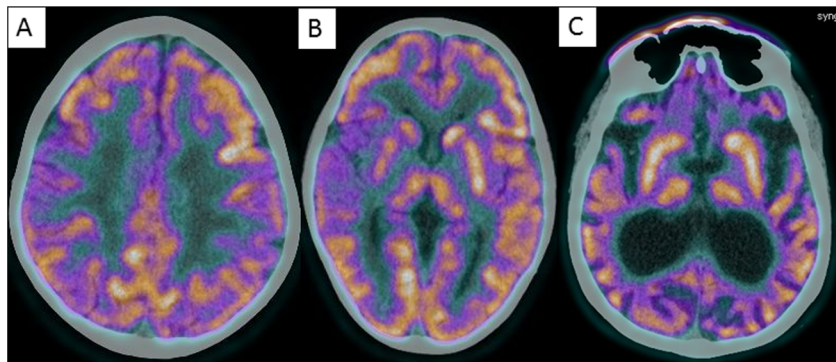


**Fig. 2** **a, b** 2/M with a history of seizures, fused F-18 FDG PET/CT images reveal patchy hypometabolism in the right frontal lobe and right basal ganglia. The child was NMDAR antibody positive. **c** 26/M with

NMDAR antibodies, fused F-18 FDG PET/CT images reveal cerebral atrophy with generalized cortical hypometabolism

showed hypermetabolism visual interpretation were 9.4/8.9 (R) and 9.3/9.3 (L) and for mesial temporal cortices, the maximum Z-scores were 16.4 (R) and 9.9 (L). Similarly, on Cortex ID, the median Z-score for hypometabolism in parietal and occipital lobes was -2.2 (R) and -2.4 (L) and -2.6 (R) and -2.4 (L) respectively. Cortex ID provides the Z-scores of the 3D stereotactic surface projection maps and the basal ganglia are not a part of standard analysis. Hypermetabolism was thus better appreciated on visual and Scenium analysis (Fig. 6) only.

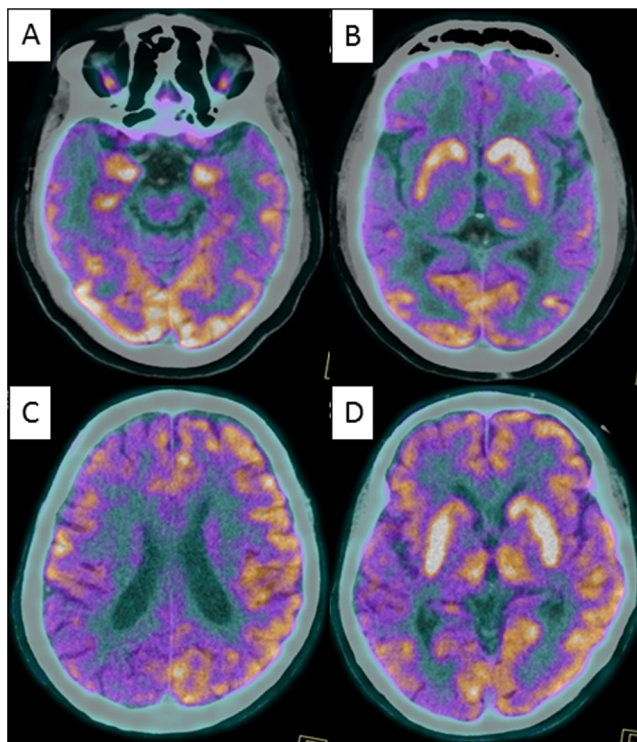


**Fig. 3** **a, b** 66/M with recent onset memory loss positive for LGI1 antibodies, fused F-18 FDG PET/CT images reveal hypermetabolism in both mesial temporal cortices and left caudate. **c, d** Fused F-18 FDG PET/CT images in a 61/M with rapidly progressive dementia and VGKC antibodies reveals hypometabolism in right cerebral hemisphere and hypermetabolism in both basal ganglia

Midbrain hypermetabolism was well appreciated visually in two patients but was not seen on semi-quantitative analysis.

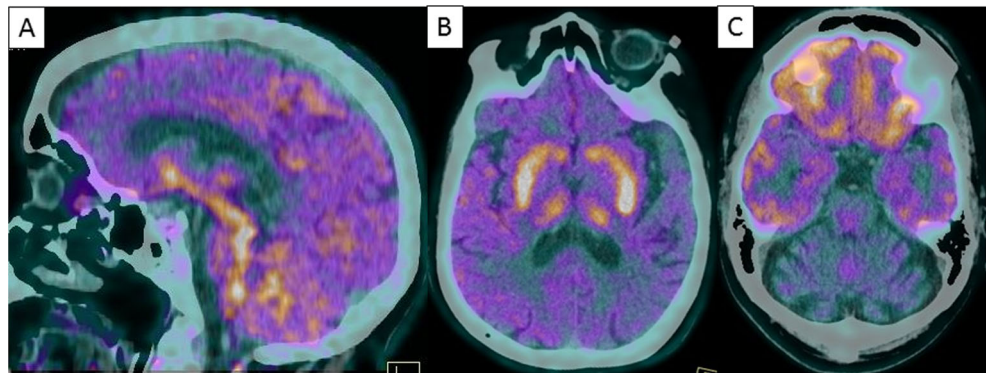
MRI had revealed signal changes suspicious of AIE in 11(45.8%) patients at the time of PET scanning, and each investigation had been reported independent of the other at the time of diagnostic work-up. The most common positive MRI finding in patients was T2/FLAIR hyperintensities in the medial temporal lobe (Fig. 7).

## Discussion

Several case reports and case series have described various patterns of metabolism on F-18 FDG PET in AIE related to specific antibody targeting sites.

NMDAR antibody encephalitis ranks among the most common forms of AIE [21]. In our series of NMDAR antibody encephalitis, various spatial distribution patterns of altered metabolism (hypermetabolism, hyper-hypometabolism, or hypometabolism) were documented on FDG PET. Hypermetabolism typically involved the basal ganglia, the mesial temporal cortices, midbrain, or basifrontal cortices (Table 1). Atypical patterns with hypermetabolism involving the lateral temporal cortices, or the basal ganglia and occipital cortices in combination were also noted. Hypometabolism in patients with NMDAR antibody encephalitis showed a parieto-occipital gradient. One patient showed a hemispheric predominance with hypometabolism involving the left cerebral hemisphere and in one patient with a delayed diagnosis there was generalized cortical hypometabolism. His MRI revealed cerebral atrophy and periventricular and perisylvian signal alterations. Thus in contrast to limbic encephalitis, where the mesial temporal structures are affected, cortical and subcortical regions in combination can be affected by NMDAR antibody encephalitis. Further, these metabolic patterns have been found to correlate more closely with the clinical picture, disease severity, and recovery after therapy than MRI findings [22, 23]. A recent review of neuroimaging studies in approximately 800 patients described the spectrum

**Fig. 4** Basal ganglia and brainstem hypermetabolism in one case of anti-GAD antibody



of FDG PET findings in NMDAR AIE [23]. On PET, an increased fronto-temporal-occipital gradient (frontotemporal glucose hypermetabolism and occipital hypometabolism) was reported. Altered metabolism was also seen in frontal, temporal, and occipital lobes; basal ganglia; cerebellum; and brainstem with lateralised effect in some patients [4, 5, 14, 15, 18, 24–27]. This review stated that abnormalities in MRI were present in 23–50% of patients that were typically discrete and non-specific [23, 28, 29]. Solnes et al. [30] reported lobar hypometabolism most commonly in the parietal and occipital lobes (on visual and quantitative analysis) in 91.3% of their patients with AIE. MRI was abnormal in 10/23 (43%) patients and their entire subset of anti-NMDAR encephalitis had normal MRI. They used Cortex ID for analysis, while our results with Scenium and Cortex ID showed a similar pattern of parieto-occipital hypometabolism. The same group also reported [31] that FDG PET was more often abnormal than initial EEG, MRI,

and CSF studies in patients with AIE. A pattern resembling the neurodegenerative patterns of dementia that have been documented in literature and accepted for differential diagnosis of dementias has also been described in older patients with NMDAR AIE [26]. It has been proposed that AIE associated with antibodies against cell surface antigens could be caused by a direct blockade of receptors or ion channels by autoantibodies. Both these pathological mechanisms may lead to a decrease in neuronal and synaptic activity and as a consequence, hypometabolism in the affected regions [32].

Our series of NMDAR AIE included five children below the age of 14 years. These children presented with seizures and extrapyramidal features. In three of these cases, hypermetabolism was present on both visual and Scenium analysis involving the basal ganglia, basal ganglia and occipital cortices, and the basifrontal cortices respectively. No ictal activity had been documented on the EEG during the FDG uptake

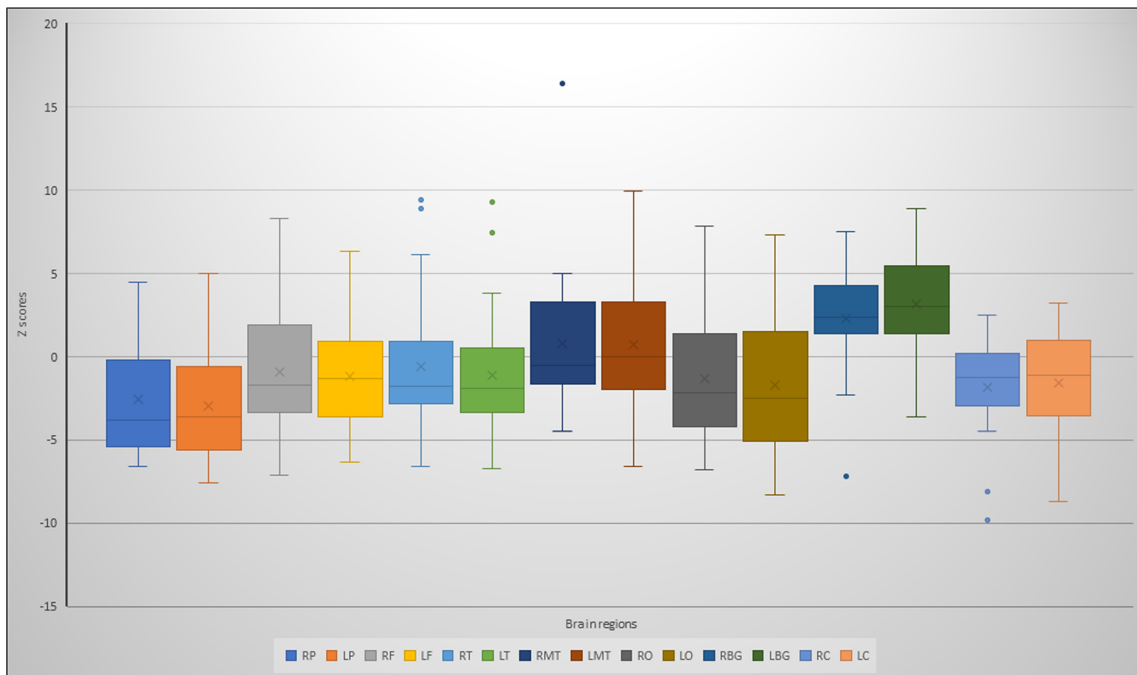
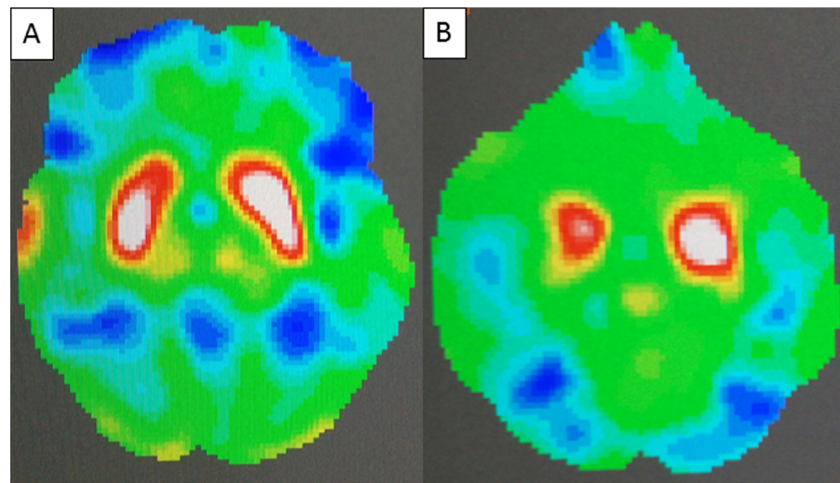


**Fig. 5** Box and whisker plot of regional Z-scores on Scenium analysis. Median, first, and third quartile and maximum and minimum Z-scores are depicted for all regions included

**Fig. 6** The voxel-based color-coded statistical analysis of significant Z-scores displaying hypermetabolism in the basal ganglia and mesial temporal cortices on Scenium analysis



phase. Initial MRI had been unremarkable in all three. In children with NMDAR AIE, early diagnosis and prompt treatment is expected to have a good prognosis, with majority of patients showing a good response to steroids and intravenous immunoglobulins [33]. Thus, presence of basal ganglia hypermetabolism should raise the suspicion of AIE in the relevant clinical setting.

Anti-LGI1 encephalitis is a newly emerging disease entity and leucine-rich glioma inactivated 1 (LGI1) is a protein associated with the VGKC complex. Both cases with FBDS had basal ganglia hypermetabolism on FDG PET on visual and Scenium Z-scores, one bilateral [20] and the other left sided which corresponded to the clinical symptomatology. Similarly cases have also been reported in literature; left basal ganglia hypermetabolism has been reported in a case with right-sided FBDS [34] and bilateral striatal hypermetabolism in a case of bilateral FBDS [35]. FBDS precedes limbic involvement in LGI1 encephalitis and immunotherapy can prevent progression to the limbic encephalitis stage. MRI at this stage is usually unremarkable [23] and PET findings can help in timely

institution of therapy. All other cases demonstrated mesial temporal hypermetabolism indicating limbic involvement. Two recent studies have shown that FDG-PET at the limbic encephalitis stage reveals altered basal ganglia metabolism in 63–70% of patients and altered temporal metabolism in 70–75% patients [36, 37]. Normal mesio-temporal glucose metabolism was correlated with better clinical outcome, whereas basal ganglia metabolism was unrelated to disease course [38]. MRI in LGI1 encephalitis presents with the typical imaging correlates of limbic encephalitis (T2/FLAIR hyperintense signal alterations in the medial temporal lobes including the hippocampus) which frequently progresses to hippocampal atrophy. Thus our series with LGI1 AIE had hypermetabolism as a predominant finding which was seen mostly involving the basal ganglia and temporal cortices and was documented on the Scenium analysis also. Wegner et al. reported hypermetabolism in the basal ganglia, cerebellum, occipital lobe, and precentral gyrus and hypometabolism in the anterior cingulate in four cases of LGI1 antibody encephalitis in comparison to normal controls [28]. This finding might partially be related to the disease stage as has been suggested by longitudinal PET investigations showing a waxing and waning of temporal PET metabolism mirroring the clinical course of disease [38].

Glutamic acid decarboxylase (GAD) is an intracellular synaptic antigen concentrated in the presynaptic terminals that can be exposed to antibodies during synaptic vesicle fusion and reuptake [39]. The presence of high titers of GAD antibody has been associated with different neurological syndromes including cerebellar ataxia and limbic encephalitis [40]. In GAD antibody encephalitis, mesial temporal and basal ganglia hypermetabolism was noted while cerebellar hypometabolism was seen in the patient who presented with symmetrical gait ataxia with isolated atrophy of cerebellar hemispheres on MRI. MRI has been found to show characteristic T2/FLAIR hyperintensities in the medial temporal lobe, the FLAIR hyperintensity values are higher than that seen

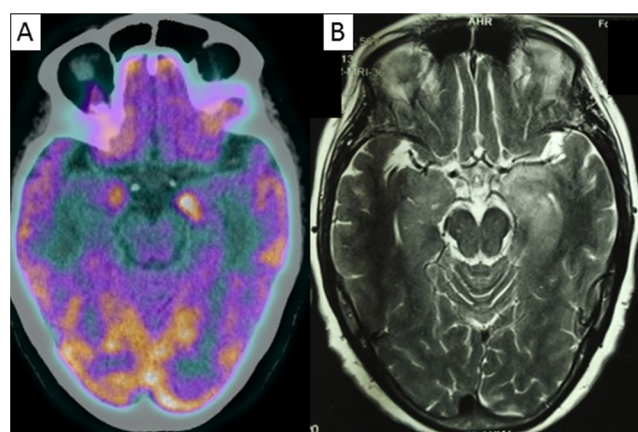


**Fig. 7** Fused FDG PET/CT images in a patient with mesial temporal hypermetabolism with corresponding axial MRI showing mesial temporal hyperintensities which is the commonest finding in AIE

with NMDA or VGKC antibodies [27]. While in GAD antibody-positive patients with cerebellar ataxia, MRI shows isolated atrophy of cerebellum [41, 42] which goes with the finding of cerebellar hypometabolism on PET.

Regional Z-score analysis using Scenium and Cortex ID was performed on an individual case basis and supported the findings of parieto-occipital hypometabolism and basal ganglia hypermetabolism (Scenium only). Hypermetabolism was seen in 16/24 patients (66%) and scenium proved a better application in patients with basal ganglia hypermetabolism. Though median Z-scores for hypermetabolism in medial and lateral temporal regions was not significant but the Z-scores in individual cases were significant on semiquantitative analysis. Midbrain hypermetabolism in two cases was better appreciated visually.

Of importance is that PET scans in all cases were done before a clinical diagnosis was established. In parallel, the MRI scans in these patients demonstrated signal changes supporting AIE in 11 patients (45.8%). Baumgartner et al. in their series found changes in 77.8% PET scans vs only 62.5% with MRI changes [4]. The kappa for overall agreement between PET and MRI for scan abnormality in encephalitis was 0.43, indicating moderate agreement [4]. Patients with negative antibody titers were positive on PET and MRI, suggesting their role in early antibody negative encephalitis. In the series by Newey et al., PET detected changes earlier than MRI in three cases [43].

Thus, FDG PET imaging in AIE represents a spectrum of various spatial distribution patterns of altered metabolism, with parieto-occipital hypometabolism and basal ganglia hypermetabolism being the most prominent abnormality. Distinct metabolic patterns which will enable characterization of specific antibody subtypes of non-paraneoplastic AIE however were not identified visually. As suggested by Morbelli et al., the availability of larger subgroups of AIE patients may allow for uncovering of sub-group-specific diagnostic potentials of FDG PET [44]. Lateral temporal hypermetabolism was unique to NMDAR AIE. Basal ganglia hypermetabolism, especially in the FBDS stage of LGI1 AIE, where MRI is usually unremarkable could have an important role to play to expedite clinical diagnosis and initiate timely therapy.

Though these observations cannot be generalized because of the small number of cases included, it definitely reiterates the emerging importance of metabolic abnormalities on FDG PET in supporting an early diagnosis of AIE.

## Conclusion

FDG PET imaging in AIE presents a spectrum of metabolic topographies with parieto-occipital hypometabolism and basal ganglia hypermetabolism being the most prominent abnormality, which along with a suggestive clinical history would

be useful for supporting a diagnosis of AIE. Visual analysis supported by Scenium is extremely useful for demonstration of the metabolic abnormality.

**Acknowledgements** The authors wish to acknowledge Mr. Rajeev Kumar, Medical Physicist, for his help in carrying out the patient studies.

**Funding** The antibody profile section of this study was funded by a grant from the Department of Biotechnology (BT/PR-3436/MED/30/651/2011), All India Institute of Medical Sciences.

### Compliance with ethical standards

**Conflict of interest** The authors declare that they have no conflict of interest.

**Ethical approval** All procedures performed in the studies involving human participants were in accordance with the ethical standards of the institutional and/or national research committee and with the 1964 Helsinki Declaration and its later amendments or comparable ethical standards. For this type of study formal consent is not required.

**Informed consent** Informed consent was obtained from all individual participants included in the study.

## References

- Graus F, Titulaer MJ, Balu R, Benseler S, Bien CG, Cellucci T, Cortese I, Dale RC, Gelfand JM, Geschwind M, Glaser CA, Honnorat J, Höftberger R, Iizuka T, Irani SR, Lancaster E, Leypoldt F, Prüss H, Rae-Grant A, Reindl M, Rosenfeld MR, Rostásy K, Saiz A, Venkatesan A, Vincent A, Wandinger KP, Waters P, Dalmau J (2016) A clinical approach to diagnosis of autoimmune encephalitis. Lancet Neurol 15(4):391–404. [https://doi.org/10.1016/S1474-4422\(15\)00401-9](https://doi.org/10.1016/S1474-4422(15)00401-9)
- Dalmau J, Rosenfeld MR (2014) Autoimmune encephalitis update. Neuro-Oncology 61:25–36
- Irani SR, Gelfand JM, Bettcher BM, Singhal NS, Geschwind MD (2014) Effect of rituximab in patients with leucine-rich glioma-inactivated 1 antibody associated encephalopathy. JAMA Neurol 71(7):896–900. <https://doi.org/10.1001/jamaneurol.2014.463>
- Baumgartner A, Rauer S, Mader I, Meyer PT (2013) Cerebral FDG-PET and MRI findings in autoimmune limbic encephalitis: correlation with autoantibody types. J Neurol 260(260):2744–2753. <https://doi.org/10.1007/s00415-013-7048-2>
- Irani SR, Bera K, Waters P, Zuliani L, Maxwell S, Zandi MS, Friese MA, Galea I, Kullmann DM, Beeson D, Lang B, Bien CG, Vincent A (2010) N-methyl-D-aspartate antibody encephalitis: temporal progression of clinical and paraclinical observations in a predominantly non-paraneoplastic disorder of both sexes. Brain 133(6): 1655–1667. <https://doi.org/10.1093/brain/awq113>
- Dalmau J, Batallar L (2006) Clinical and immunological diversity of limbic encephalitis: a model for paraneoplastic neurologic disorders. Hematol Oncol Clin North Am 20(6):1319–1335. <https://doi.org/10.1016/j.hoc.2006.09.011>
- Annes BM, Vitaliani R, Taylor RA, Liebeskind DS, Voloschin A, Houghton DJ, Galetta SL, Dichter M, Alavi A, Rosenfeld MR, Dalmau J (2005) Treatment-responsive limbic encephalitis identified by neuropil antibodies: MRI and PET correlates. Brain 128(8): 1764–1777. <https://doi.org/10.1093/brain/awh526>

8. Scheid R, Lincke T, Voltz R, von Cramon DY, Sabri O (2004) Serial 18F-fluoro-2-deoxy-D-glucose positron emission tomography and magnetic resonance imaging of paraneoplastic limbic encephalitis. *Arch Neurol* 61(11):1785–1789. 2. <https://doi.org/10.1001/archneur.61.11.1785>
9. Provenzale JM, Barboriak DP, Coleman RE (1998) Limbic encephalitis: comparison of FDG-PET and MR imaging findings. *Am J Roentgenol* 170(6):1659–1660. 3. <https://doi.org/10.2214/ajr.170.9609193>
10. Hoffmann LA, Jarius S, Pellkofer HL et al (2008) Anti-Ma and anti-Ta associated paraneoplastic neurological syndromes: 22 newly diagnosed patients and review of previous cases. *J NeurolNeurosurgPsychia* 79:767–773
11. Blanc F, Ruppert E, Kleitz C, Valenti MP, Cretin B, H umbel RL, Honnorat J, Namer IJ, Hirsch E, Manning L, de Seze J (2009) Acute limbic encephalitis and glutamic acid decarboxylase antibodies: a reality? *J Neurol Sci* 287(1-2):69–71. <https://doi.org/10.1016/j.jns.2009.09.004>
12. Greiner H, Leach JL, Lee KH, Krueger DA (2011) Anti-NMDA receptor encephalitis presenting with imaging findings and clinical features mimicking Rasmussen syndrome. *Seizure* 20(3):266–270. <https://doi.org/10.1016/j.seizure.2010.11.013>
13. Pillai SC, Gill D, Webster R et al (2010) Cortical hypometabolism demonstrated by PET in relapsing NMDA receptor encephalitis. *PediatrNeurol* 43:217–220
14. Maqbool M, Oleske DA, Huq AH et al (2011) Novel FDG-PET findings in NMDA receptor encephalitis: a case based report. *J Child Neurol* 26(10):1325–1328. 2752. <https://doi.org/10.1177/0883073811405199>
15. Caballero PE (2011) Fluorodeoxyglucose positron emission tomography findings in NMDA receptor antibody encephalitis. *ArqNeuropsiquiatr* 69:409–410. 13
16. Padma S, Sundaram PS, Marmattom BV (2011) PET/CT in the evaluation of anti-NMDA-receptor encephalitis: what we need to know as a NM physician. *Ind J Nucl Med* 26(2):99–101. <https://doi.org/10.4103/0972-3919.90262>
17. Maeder-Ingvär M, Prior JO, Irani SR, Rey V, Vincent A, Rossetti AO (2011) FDG-PET hyperactivity in basal ganglia correlating with clinical course in anti-NDMA-R antibodies encephalitis. *J NeurolNeurosurg Psychiatry* 82(2):235–236. <https://doi.org/10.1136/jnnp.2009.198697>
18. Mohr BC, Minoshima S (2010) F-18 fluorodeoxyglucose PET/CT findings in a case of anti-NMDA receptor encephalitis. *ClinNucl Med* 35:461–463
19. Rey C, Koric L, Guedj E, Felician O, Kaphan E, Boucraut J, Ceccaldi M (2012) Striatal hypermetabolism in limbic encephalitis. *J Neurol* 259(6):1106–1110. <https://doi.org/10.1007/s00415-011-6308-2>
20. Dash D, Tripathi M, Ihtisham K, Tripathi M (2016) LGI1 encephalitis: a disease of jerks and confusion. *BMJ Case Rep*. <https://doi.org/10.1136/bcr-2016-217083>
21. Granerod J, Ambrose HE, Davies NW, Clewley JP, Walsh AL, Morgan D et al (2010) Causes of encephalitis and differences in their clinical presentations in England: a multicentre population-based prospective study. *Lancet Infect Dis* 10(12):835–844. [https://doi.org/10.1016/S1473-3099\(10\)70222-X](https://doi.org/10.1016/S1473-3099(10)70222-X)
22. Vollmer TL, McCarthy M (2016) Autoimmune encephalitis: a more treatable tragedy if diagnosed early. *Neurology* 86(18):1655–1656. <https://doi.org/10.1212/WNL.0000000000002641>
23. Heine J, Pruss H, Bartsch T, Ploner CJ, Paul F, Finke C (2015) Imaging of autoimmune encephalitis-relevance for clinical practice and hippocampal function. *Neuroscience* 309:68–83. <https://doi.org/10.1016/j.neuroscience.2015.05.037>
24. Leyboldt F, Buchert R, Kleiter I, Marienhagen J, Gelderblom M, Magnus T, Dalmau J, Gerloff C, Lewerenz J (2012) Fluorodeoxyglucose positron emission tomography in anti-N-
25. Vitaliani R, Mason W, Ances B, Zwerdling T, Jiang Z, Dalmau J (2005) Paraneoplastic encephalitis, psychiatric symptoms and hypoventilation in ovarian teratoma. *Ann Neurol* 58(4):594–604. <https://doi.org/10.1002/ana.20614>
26. Fischer RE, Patel NR, Lai EC, Schulz PE (2012) Two different FDG brain PET metabolic patterns in autoimmune limbic encephalitis. *Clin Nucl Med* 37(9):e213–e218. <https://doi.org/10.1097/RLU.0b013e31824852c7>
27. Wegner F, Wilke F, Raab P, Tayeb S, Boeck A, Haense C et al (2014) Anti-leucine rich glioma inactivated 1 protein and anti-N-methyl-D-aspartate receptor encephalitis show distinct patterns of brain glucose metabolism in F-18 Fluoro-2-deoxyglucose positron emission tomography. *BMC Neurol* 14(1):136. <https://doi.org/10.1186/1471-2377-14-136>
28. Dalmau J, Lancaster E, Martinez-Hernandez E, Rosenfeld MR, Balice-Gordon R (2011) Clinical experience and laboratory investigations in patients with anti-NMDAR encephalitis. *Lancet Neurol* 10(1):63–74. [https://doi.org/10.1016/S1474-4422\(10\)70253-2](https://doi.org/10.1016/S1474-4422(10)70253-2)
29. Titulaer MJ, McCracken L, Gabilondo I, Armangue T, Glaser C, Iizuka T et al (2013) Treatment and prognostic factors for long-term outcome in patients with anti-NMDA receptor encephalitis: an observational cohort study. *Lancet Neurol* 12(2):157–165. [https://doi.org/10.1016/S1474-4422\(12\)70310-1](https://doi.org/10.1016/S1474-4422(12)70310-1)
30. Solnes LB, Jones KM, Rowe SP, Pattanayak P, Nalluri A, Venkatesan A, Probasco JC, Javadi MS (2017) Diagnostic value of F-18 FDG PET/CT versus MRI in the setting of antibody specific autoimmune encephalitis. *JNM* 58(8):1307–1313. <https://doi.org/10.2967/jnumed.116.184333>
31. Probasco JC, Solnes LB, Nalluri A, Cohen J, Jones KM, Zan E et al (2017) Abnormal brain metabolism on FDG PET/CT is a common early finding in autoimmune encephalitis. *Neurol Neuroimmunol Neuroinflamm* 4(4):e352. <https://doi.org/10.1212/NXI.0000000000000352>
32. Hughes EG, Peng X, Gleichman AJ, Lai M, Zhou L, Tsou R, Parsons TD, Lynch DR, Dalmau J, Balice-Gordon RJ (2010) Cellular and synaptic mechanisms of anti-NMDA receptor encephalitis. *J Neurosci* 30(17):5866–5875. <https://doi.org/10.1523/JNEUROSCI.0167-10.2010>
33. Chakrabarty B, Tripathi M, Gulati S, Yoganathan S, Pandit AK, Sinha A, Rathi BS (2014) Pediatric anti-methyl-D-aspartate (NMDA) receptor encephalitis: experience of a tertiary care teaching centre from north India. *J Child Neurol* 29(11):1453–1459. <https://doi.org/10.1177/0883073813494474>
34. Boesebeck F, Schwarz O, Dohmen B, Graef U, Vestring T, Kramme C, Bien CG (2013) Faciobrachial dystonic seizures arise from cortico-subcortical abnormal brain areas. *J Neurol* 260(6):1684–1686. <https://doi.org/10.1007/s00415-013-6946-7>
35. Fidzinski P, Jarius S, Gaebler C, Boegner F, Nohr R, Ruprecht K (2014) Faciobrachial dystonic seizures and antibodies to LGI1 in a 92-year old patient: a case report. *J Neurol Sci* 347(1-2):404–405. <https://doi.org/10.1016/j.jns.2014.10.026>
36. Irani SR, Michell AW, Lang B, Pettingill P, Waters P, Johnson MR, Schott JM, Armstrong RJE, S. Zagami A, Bleasel A, Somerville ER, Smith SMJ, Vincent A (2011) Faciobrachial dystonic seizures precede IgG antibody limbic encephalitis. *Ann Neurol* 69(5):892–900. <https://doi.org/10.1002/ana.22307>
37. Shin Y-W, Lee S-T, Shin J-W, Moon J, Lim J-A, Byun J-I, Kim TJ, Lee KJ, Kim YS, Park KI, Jung KH, Lee SK, Chu K (2013) VGKC complex/LGI1 antibody encephalitis: clinical manifestations and response to immunotherapy. *J Neuroimmunol* 265(1-2):75–81. <https://doi.org/10.1016/j.jneuroim.2013.10.005>
38. Park S, Choi H, Cheon GJ, Wook Kang K, Lee DS (2015) F-18 FDG PET/CT in anti-LGI1 encephalitis: initial and follow-up

- findings. *Clin Nucl Med* 40(2):156–158. <https://doi.org/10.1097/RLU.00000000000000546>
39. Lancaster E, Dalmau J (2012) Neuronal autoantigens-pathogenesis, associated disorders and antibody testing. *Nat Rev Neurol* 8(7):380–390. <https://doi.org/10.1038/nrneurol.2012.99>
40. Saiz A, Blanco Y, Sabater L, Gonzalez F, Bataller L, Casamitjana R et al (2008) Spectrum of neurological syndromes associated with glutamic acid decarboxylase antibodies: diagnostic clues for this association. *Brain* 131(10):2553–2563. <https://doi.org/10.1093/brain/awn183>
41. Honnorat J, Saiz A, Giometto B, Vincent A, Brieva L, Andreas C et al (2001) Cerebellar ataxia with anti-glutamic acid decarboxylase antibodies. *Arch Neurol* 58(2):225–230. <https://doi.org/10.1001/archneur.58.2.225>
42. Arino H, Gresa-Arribas N, Blaco Y, Martinez-Hernandez E, Sabater L, Petit-Pedrol M et al Cerebellar ataxia and glutamic acid decarboxylase antibodies: immunologic profile and long-term effect of immunotherapy. *JAMA Neurol* 71:1009–1016
43. Newey CR, Sarwal A, Hantus S (2016) F-18 Fluoro-deoxy-glucose positron emission tomography scan should be obtained early in cases of autoimmune encephalitis. *Autoimmune Dis* 2016: 9450452. <https://doi.org/10.1155/2016/9450452>
44. Morbelli S, Arbizu J, Booji J, Chen MK, Chetelat G, Cross DJ et al (2017) The need for standardization and of large clinical studies in an emerging indication of F-18 FDG PET: the autoimmune encephalitis. *Eur J Nucl Med Mol Imaging* 44(3):353–357. <https://doi.org/10.1007/s00259-016-3589-9>